Motion Analysis of Objects Carried by Multiple Cooperating Manipulators with Frictional Contacts

Jihong Lee* and Wonhee Lee**

Department of Mechatronics Engineering, Chungnam National University, Daejeon , Korea
Tel : +82-42-821-7783; E-mail: (*)jihong@cnu.ac.kr, (**) s_wonhee@cnu.ac.kr

Abstract: In this paper a mathematical framework for deriving acceleration bounds from given joint torque limits of multiple cooperating robots are described. Especially when the different frictional contacts for every contact are assumed and the torque limits are given in 2-norm sense, we show that the resultant geometrical configuration for the acceleration is composed of corresponding parts of ellipsoids. Since the frictional forces at the contacts are proportional to the normal squeezing forces, the key points of the work includes how to determine internal forces exerted by each robot in order not to cause slip at the contacts while the object is carried by external forces. A set of examples composed of two robot systems are shown with point-contact-with-friction model and insufficient or proper degree of freedom robots.

Keywords: friction coefficient, multiple robots, contact conditions, ellipsoid, dynamic constraints, dynamic manipulability

1. INTRODUCTION

Many studies handling robot motion capabilities given actuator constraints are included in the research area of so-called robotic manipulability. In recent, many studies of multi-arm cooperative manipulations which provide flexibility and versatility in task execution have been performed [1-2]. The studies for multiple cooperating robot system are largely classified into robot kinematics analysis (handling velocities) kinematics [3-6] and dynamics analysis (handling forces or accelerations) [7-9].

Many kinematical analyses have been made along the geometry so-called manipulability ellipsoid [4, 10] which is derived when the joint constraints are given in 2-norm sense [1] or along the geometry of polytope which is derived when the joint constraints are given in infinity-norm sense [6, 11]. Also, many works have handled such contact conditions as hard finger, soft finger, and very soft finger [6]. Especially when dynamic situations are under consideration in practical problem, contact conditions play important roles in the manipulability. The contact condition determines the convey-ability of force and moment from robot end-effecters to the object grasped by the robots. Since the contact friction, however, is difficult to be included in the usual dynamics of both robots and object to be carried, one can hardly find any works including contact friction in the analysis of robot dynamic manipulability. Since each robot can only push the object in general frictional contacts, the conventional techniques assuming that robots can pull the object cannot be applied in this situation also that the force exerted by each robot is composed of external force and internal force. The former is transferred to the object and carries the object while the latter is defined as a portion of total force exerted by robot hand which does not affect the object motion but just squeezes it.

The goal of this study is to derive the acceleration bound of object carried by the cooperating robots with limited torque bounds through frictional contacts. The joint constraint taken in this paper is defined in 2-norm sense which reflects the energy of the system. To be specific, under the assumption that the contact geometries and friction coefficients are known, we calculate minimum internal forces needed to generate frictional forces required in carrying the object while the robot system carries the object. And then we include the internal force to the robot dynamics to decide which parts of torque contribute to carrying object and sustaining the frictional forces required not to slip the object. Finally we figure out how much and which way the contact frictions change the geometry of usual manipulability ellipsoid with different frictional coefficients at every contact.

This work was supported by grant No. R05-2003-000-10215-0 from Korea Science & Engineering Foundation.

II. FRICTION CONE AND INTERNAL FORCE

1. Friction cone

Let's assume m robots make frictional point contact with an object and also assume each robot can only push the object. Then, the maximum static frictional condition is given as

$$\cos\theta_i \geq \frac{1}{\sqrt{1+\mu_i^2}} \equiv \eta_i \tag{1}$$

where μ_i is maximum static frictional coefficient between the object and the i-th robot. We call the shaded area in Fig 1 as friction cone [1].

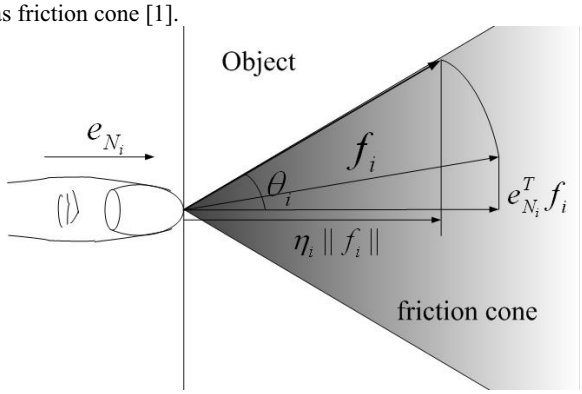

Fig. 1 Static frictional constraints

2. Internal force

When m robots apply forces $F = \left[f_1^T \; f_2^T \cdots f_m^T\right]^T$ to one object, the resultant force and moment Q of the object is given as $Q = WF$ with grasp matrix W. In reverse relation, we get

$$F = W^{\#}Q + \left(E - W^{\#}W\right)V \tag{2}$$

where E is identity matrix and V is arbitrary vector. Note $W^{\#}Q$ is portion of force that contributes to object motion

while $\left(E - W^{\#}W\right)V$ is portion of force that does not contribute to object motion. In this paper, we call the former 'external force' and the latter 'internal force'. Also, in individual robot, the force f_i exerted by the robot is decomposed into external force f_i^E and internal force f_i^I:

$$f_i = f_i^E + f_i^I . \tag{3}$$

To carry the object without slip, every robot exerts its force f_i along direction inside of friction cone. Referring to Fig. 2, with given external force determined from the object motion there are lots of ways to make the total force align inside friction cone with any internal forces satisfying

$$WF^I = 0 \tag{4}$$

where F^I is $\left[\left(f_1^I\right)^T \left(f_2^I\right)^T \cdots \left(f_m^I\right)^T\right]^T$.

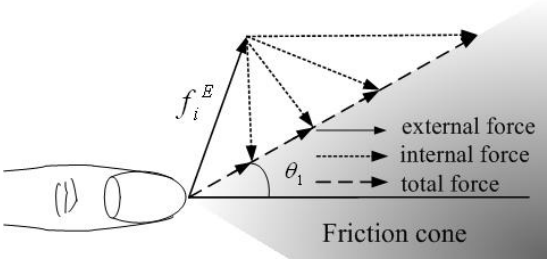

Fig. 2 Associations of internal force and external force

In this work we adopt a rule that selecting internal forces to make the total force on the boundary of friction cone.

3. Dividing acceleration workspace by friction cones and contact geometry

The key idea of this work is to apply different elliptic geometry to every divided acceleration workspace according to the maximum static frictional condition and contact geometry. The former is rewritten as

$$C_i = \left\{ f_i \mid e_{Ni}{}^T f_i \geq \eta_i \left\| f_i \right\| \right\}, \tag{5}$$

where e_{Ni} is normal vector of contact point i while the latter is rewritten as

$$P_i = \left\{ f_i \mid e_{Ni}{}^T f_i \geq 0 \right\}. \tag{6}$$

When multiplied by object mass, the object acceleration becomes total force exerted to object. Since the acceleration workspace is equivalent to the total force exerted to object, we apply the rules that divide the force workspace to the acceleration workspace and from now on we handle only acceleration workspace. Note that for every divided workspace different rules for introducing internal forces and different rules for distributing the force required to move the object are specified. An example for dividing the acceleration workspace by (5) and (6) is shown in Fig, 3.

As can be seen in Fig. 3, the boundary described by dashed line is determined by (5), and the boundary described by dash-dot line is determined by (6). Note that the (6) implies that the robots con only push the object. Based on the observation there are 8 possible regions: region1 = $\overline{C}_1 P_1 \overline{C}_2 \overline{P}_2$, region2 = $C_1 P_1 \overline{C}_2 \overline{P}_2$, region3 = $\overline{C}_1 P_1 \overline{C}_2 \overline{P}_2$, region4 = $\overline{C}_1 \overline{P}_1 \overline{C}_2 P_2$, region5 = $\overline{C}_1 \overline{P}_1 \overline{C}_2 P_2$, region6 = $\overline{C}_1 \overline{P}_1 C_2 P_2$, region7 = $\overline{C}_1 \overline{P}_1 \overline{C}_2 P_2$ and region8 = $\overline{C}_1 P_1 \overline{C}_2 \overline{P}_2$. For example in region 3, only robot 1 can push the object (P_1), robot 2 can't push the object ($\overline{P}_2$) and internal force for two robots are required since region 3 is outside of two friction cone ($\overline{C}_1 \overline{C}_2$).

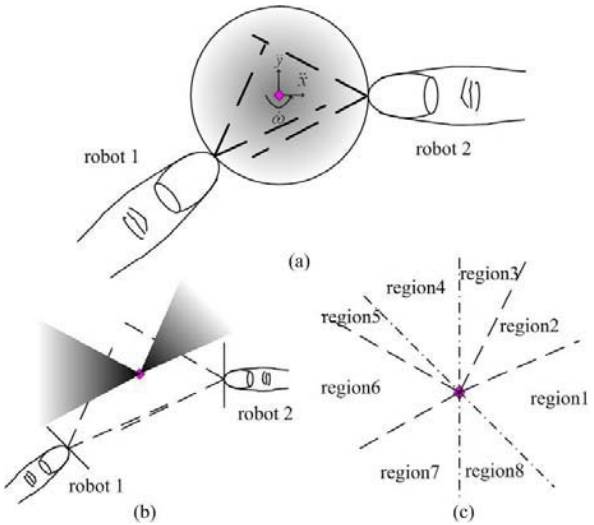

Fig. 3 Divided workspace (a) contact configuration
(b) The friction cones depicted in mass center
(c) The workspace divided by Eq. (5) and (6)

III. Classifying acceleration workspace

In this section, we describe how to class the workspace according to whether the internal forces are required or not and the object motion can be realized a single robot or not. When we denote each robot's force as

$$F = \begin{bmatrix} f_1 \\ \vdots \\ f_i \\ \vdots \\ f_m \end{bmatrix} = \begin{bmatrix} f_1^E \\ \vdots \\ f_i^E \\ \vdots \\ f_m^E \end{bmatrix} + \begin{bmatrix} f_1^I \\ \vdots \\ f_i^I \\ \vdots \\ f_m^I \end{bmatrix} \equiv F^E + F^I, \tag{7}$$

The problem is summarized as:

[Problem] When Q is specified, find each f_i^E and f_i^I satisfying $Q = WF^E$ and $WF^I = 0$, and locating each robot's total force $f_i = f_i^E + f_i^I$ on or inside of corresponding robot's friction cone.

1.1 Class A: No internal forces required

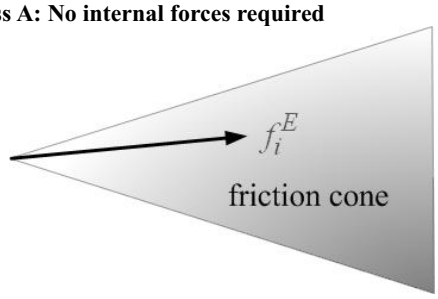

Fig. 4 Force relationship of class A

When the force exerted to the object is in a friction cone, the robot system always exerts the force without any frictional force, i.e., no internal force. In this case it is natural that a robot whose friction cone contains the total force in its region contributes to all the force:

$$F = f_i^E \tag{8}$$

1.2 Class B. Single robot covers object motion

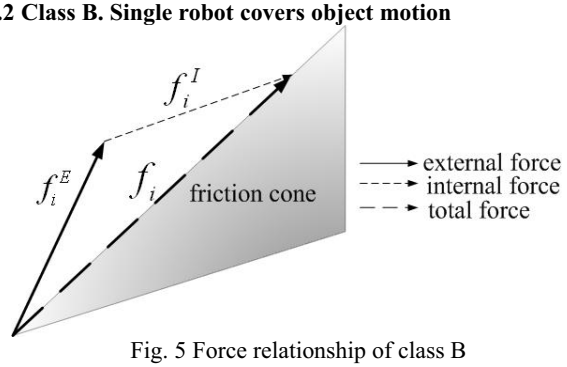

Fig. 5 Force relationship of class B

This case implies force exerted to object is not included in any friction cones, and so internal forces are required to generate the needed frictional forces. And in this case the force exerted to the object is generated by single robot that can push the object. Note that the internal forces play roles of pushing the total force of the specified robot into its friction cone.

$$F = \begin{bmatrix} f_1 \\ \vdots \\ f_i \\ \vdots \\ f_m \end{bmatrix} = \begin{bmatrix} f_1^I \\ \vdots \\ f_i^E + f_i^I \\ \vdots \\ f_m^I \end{bmatrix} \tag{9}$$

1.3 **Class C. Multiple robots contribute to object motion**

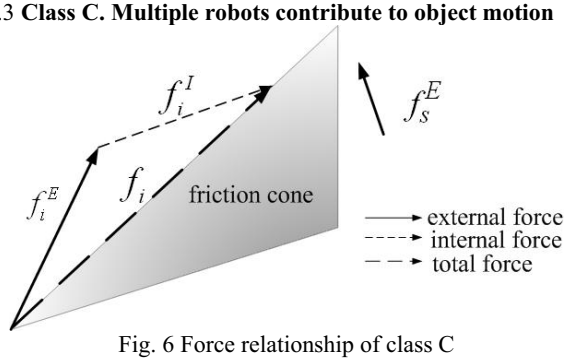

Fig. 6 Force relationship of class C

The situation of this class is little bit complex compared with other classes. The problem is that the required external force is not generated by single robot and to generate the external force some robots require internal forces to generated friction force. to calculate each robot's internal force so that each robot's total force is located on or inside of each robot's friction cone.

According to the number of robots the solution of the above problem is not uniquely determined. To be specific, finding external force from object force is related with force distribution or load distribution. Among many selection rules, distributing external force according to friction coefficient is adopted in this work, which will be described in case studies. In conclusion, some robots' external forces that belong to set S are described in terms of their internal force:

$$f_S^E = \mu_s(e_{TS}) g_{NS} f_S^I, s \in S = \{i \mid Q \subset \cup P_i\} \tag{10}$$

where μ_S is maximum static frictional coefficient between the object and the contact point S, g_{NS} is the matrix that calculates magnitude of internal force of robot S, and e_{TS} is the unit vector along tangential direction of contact point S.

Example 1: Let's consider an example of Fig. 6. Eq. (4) is extracted as $f_1^I + f_2^I + \cdots + f_m^I = 0$. Let's define size and direction of internal force of robot i as $\left|f_i^I\right|$ and e_i^I respectively. Then front equation is rearranged by $\left|f_1^I\right| e_1^I + \left|f_2^I\right| e_2^I + \cdots + \left|f_m^I\right| e_m^I = 0$. If number of robot is changed, number of internal force is changed such that direction of internal force is changed. Though the number of robot isn't changed, the direction e_i^I of internal force of robot i is various as seen in Fig. 2, too.

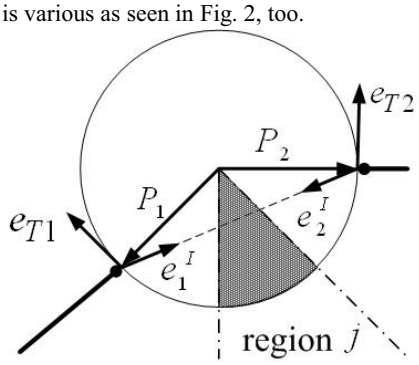

Fig. 7 An example of class C situation (Shaded area)

In this paper, when two robots carry one object in cooperative way as Fig. 7, we determine direction of internal force, get internal force and external force, and represent force of all robots as external force of specific robot.

From position vector p_i between robot i and the mass center of object, we define direction of internal force as

$$e_1^I = \frac{p_2 - p_1}{|p_2 - p_1|}, \quad e_2^I = -e_1^I. \tag{11}$$

With the direction vectors of internal forces, internal forces are determined from Fig. 7. Therefore, from an observation based on geometry, we get following equations.

$$f_1^I = M_{1j} f_1^E \tag{12}$$

$$f_2^I = -M_{1j} f_1^E \tag{13}$$

And, finally we get the external force of robot 2 as

$$f_2^E = -\mu_2(e_{T2}) g_{N2} M_{1j} f_1^E \tag{14}$$

where $g_{N2} = [1 \ 0]$. Note that external forces and internal forces of every robot are expressed by external force of specific robot (robot 1 in this example).

IV. Dynamic Equation of Multiple Robot Systems

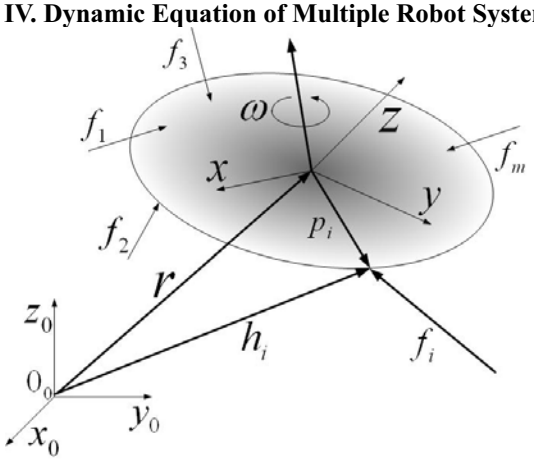

Fig. 8 Multiple-arm cooperating robot system

1. Acceleration relationships between robots and object

Let r be a vector from the origin of the absolute coordinates to the mass center of the object and h_i be a position vector from base axis to end-effecter of robot i. Then one gets $r + p_i = h_i$. When we assume point-contact-with-friction model [6] and stationary object ($\omega = 0$), we have

$$\dot{h}_i = \omega \times p_i + \dot{r} = \dot{r} \tag{15}$$

$$\ddot{h}_i = \dot{\omega} \times p_i + \ddot{r} \tag{16}$$

where $p_i = \begin{bmatrix} p_{ix} & p_{iy} & p_{iz} \end{bmatrix}^T$ in 3-dimensional case. From (16) we have

$$\ddot{h}_i = \begin{bmatrix} E_3 & -P_i \end{bmatrix} \begin{bmatrix} \ddot{r} \\ \dot{\omega} \end{bmatrix} = \begin{bmatrix} E_3 & -P_i \end{bmatrix} \ddot{u} = B_i \ddot{u} \tag{17}$$

with $P_i = \begin{bmatrix} 0 & -p_{iz} & p_{iy} \\ p_{iz} & 0 & -p_{ix} \\ -p_{iy} & p_{ix} & 0 \end{bmatrix}$ in 3-dimensional case

Let $\dot{\rho}_i$ be angular acceleration of the end-effecter of robot i. Then both the position of the end-effecter and orientation of the end-effecter in the Cartesian coordinates are x. When the robots and the object are stationary ($\dot{q} = 0$), we have $\ddot{x} = J\ddot{q}$ from $\dot{x}_i = J_i \dot{q}_i$ [1]. When all robots have as many degrees of freedom as necessary arbitrary position/orientation in the task space, J_i in $\dot{x}_i = J_i \dot{q}_i$ is invertible, so one has

$$\ddot{q}_i = J_i^{-1} \begin{bmatrix} \ddot{h}_i \\ \dot{\rho}_i \end{bmatrix} = J_i^{-1} \begin{bmatrix} B_i \ddot{u} \\ \dot{\rho}_i \end{bmatrix} \equiv \begin{bmatrix} D_{i,1} B_i & D_{i,2} \end{bmatrix} \begin{bmatrix} \ddot{u} \\ \dot{\rho}_i \end{bmatrix} \tag{18}$$

Since angular acceleration ($\dot{\rho}_i$) is irrelevant to object motion we set $\dot{\rho}_i$ as free variable in Eq. (16).

2. Force relationships between robots and object

Let's derive external force and internal force of all robots to external force of specific robot f_q^E as seen in Eqs. (12) ~ (14).

$$f_i^I = M_{ij} f_q^E, \quad f_2^I = -M_{ij} f_q^E, \quad f_i^E = H_{ij} f_q^E \tag{19}$$

For case class A, all M_{ij} and H_{ij} are zero matrix when i isn't q, only H_{ij} is identity matrix and others are zero matrix when i is q. For class B, M_{ij} isn't always zero matrix and H_{ij} is identity matrix when i is q. M_{ij} and H_{ij} are zero matrix when i isn't q. For class C, all M_{ij} and H_{ij} aren't zero matrix. Then total force of robot i is represented as

$$f_i = f_i^E + f_i^I = \begin{bmatrix} H_{ij} + M_{ij} \end{bmatrix} f_q^E \equiv K_{ij} f_q^E. \tag{20}$$

At point-contact-with-friction model, only forces (not torques) can be exerted [6] such that the resultant force and moment Q of the object is rearranged as

$$Q = \sum_{i=1}^{m} \begin{bmatrix} E_s \\ P_i^T \end{bmatrix} f_i = \sum_{i=1}^{m} \begin{bmatrix} E_s \\ P_i^T \end{bmatrix} K_{ij} f_q^E \equiv \sum_{i=1}^{m} W_{ij} f_q^E \equiv W_j f_q^E \tag{21}$$

where E_s is $s \times s$ identity matrix. Note W_j isn't square matrix so it isn't invertible. If we multiply both sides of Eq. (21) by selection matrix H which makes W_j a square matrix, one gets

$$HQ = (HW_j) f_q^E. \tag{22}$$

We multiply both sides of object dynamics [11] by selection matrix H.

$$H\left(I_0 \ddot{u} + Q_0\right) = HQ \tag{23}$$

where I_0 is inertia tensor of the object, Q_0 is a term that includes gravity effect and Coriolis force, and Q is the resultant force and moment at the mass center of object. From Eqs. (22) ~ (23), f_q^E is defined as

$$f_q^E = \begin{bmatrix} HW_j \end{bmatrix}^{-1} H(I_0 \ddot{u} + Q_0) \tag{24}$$

We assume that gravity and Coriolis force is neglected, so Eq. (24) is rewritten as

$$f_q^E = \begin{bmatrix} HW_j \end{bmatrix}^{-1} H I_0 \ddot{u} \tag{25}$$

3. Connecting dynamic equation of object and robot

The well-known dynamic equations of each robot are described as

$$\tau_i = M_i \ddot{q}_i + J_i^T F_i + V_i \, (i = 1,2,\cdots,m) \tag{26}$$

where M_i is inertia term, J_i is Jacobian matrix, $F_i = \begin{bmatrix} f_i^T & n_i^T \end{bmatrix}^T$ is force on end-effecter of robot i, and V_i includes Coriolis force, centrifugal force and gravity term. $J_i^T F_i$ is decomposed as:

$$J_i^T F_i = J_i^T \begin{bmatrix} f_i \\ n_i \end{bmatrix} \equiv S_i \begin{bmatrix} f_i \\ n_i \end{bmatrix} = \begin{bmatrix} S_{i,1} K_i & S_{i,2} \end{bmatrix} \begin{bmatrix} f_q^E \\ n_i \end{bmatrix} \tag{27}$$

At point-contact-with-friction model, we set n_i is zero and putting (17), (25) and (27) into (26) and one gets as:

$$\tau_i = \begin{bmatrix} M_i D_{i,1} B_i + S_{i,1} K_j \left(HW_j\right)^{-1} H I_0 & D_{i,2} \end{bmatrix} \begin{bmatrix} \ddot{u} \\ \dot{\rho}_i \end{bmatrix} \tag{28}$$

Eq. (28) is used as dynamic equation in class A, class B, and class C.

V. CASE STUDIES

1. Case study I

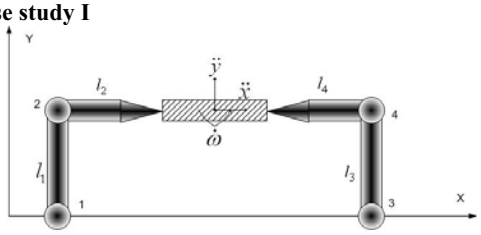

Fig. 9 Robot configuration of case I

Let's consider the system consist of two two-link limbs grasping an object as Fig. 9. Then the coordinates of the object are described in terms of $\ddot{x}$, $\ddot{y}$ and $\dot{\omega}$ while each robot has only two degrees of freedom, this case is the insufficient degree of freedom case.

From Eqs. (5) ~ (6), each workspace of Fig. 10 is described as region1 = $C_1 P_1 \overline{C}_2 \overline{P}_2$, region2 = $\overline{C}_1 P_1 \overline{C}_2 \overline{P}_2$, region3 = $\overline{C}_1 \overline{P}_1 \overline{C}_2 P_2$, region4 = $\overline{C}_1 \overline{P}_1 C_2 P_2$, region5 = $\overline{C}_1 \overline{P}_1 \overline{C}_2 P_2$ and region6 = $\overline{C}_1 P_1 \overline{C}_2 \overline{P}_2$.

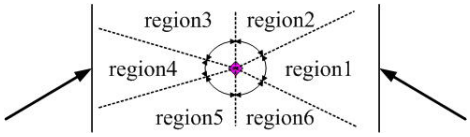

Fig. 10 the divided workspace of case I

When the configuration and parameters of robots are given at $q_1 = 90^\circ$, $q_2 = -90^\circ$, $q_3 = 90^\circ$, $q_4 = 90^\circ$, $m_{1,2,3,4} = 1$, $l_{1,2,3,4} = 1, m_0 = 1$, and $l_0 = 1$, in Fig. 11~12 both (a) and (b) show the acceleration bounds from Eq. (32). Linear acceleration of the object at left side and angular acceleration of the object are shown at right side. Both region1 and region4 of Fig.10 are following class A and others of Fig.10 are following either class B or class C. We get Fig.11, when region2, region3, region5, and region 6 are following class B, and we get Fig.12, when they are following class C. For line (b) of Fig.12, upper left direction is larger than the right side in acceleration of mass center of the object because left frictional coefficient is larger than right frictional coefficient.

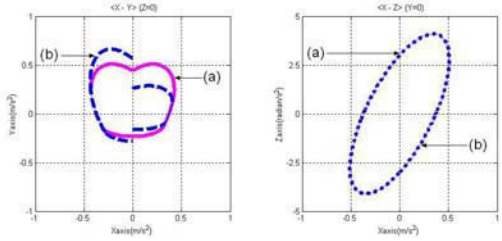

Fig. 11 Manipulability ellipsoid using class A and class B in Fig. 9
(a) Frictional contact with $\mu_1 = 0.5, \mu_2 = 0.5$
(b) Frictional contact with $\mu_1 = 0.3, \mu_2 = 0.7$

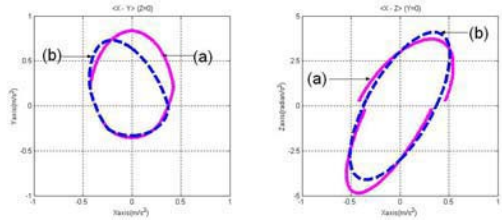

Fig. 12 Manipulability ellipsoid using class A and class C in Fig. 9
(a) Frictional contact with $\mu_1 = 0.5, \mu_2 = 0.5$
(b) Frictional contact with $\mu_1 = 0.1, \mu_2 = 0.9$

2. Case Study II

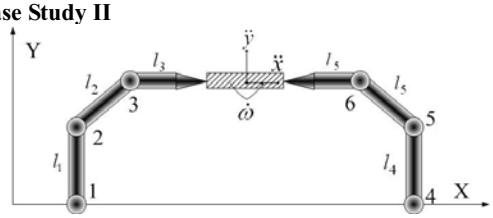

Fig. 13 Robot configuration of case II

In this example, we consider the two three-link limbs system as Fig. 13. Since the coordinates of the object are described in terms of $\ddot{x}$, $\ddot{y}$ and $\dot{\omega}$, and each robot has three degrees of freedom, so this case is the proper degree of freedom case. When the robot configurations of $q_1 = 90^\circ, q_2 = -45^\circ, q_3 = -45^\circ, q_4 = 90^\circ, q_5 = 45^\circ$, $q_6 = 45^\circ$, $m_{1,2,3,4,5,6} = 1$, $l_{1,2,3,4,5,6} = 1$, $m_o = 1$ and $l_o = 1$ are given, this system is proper D.O.F. such that we use Eq. (26) and we get the result of Fig. 14~15.

If number of link of robot is increased, force to move robot itself which conforms to $M_i \ddot{q}_i$ in Eq. (24) is increased, too. Therefore force to move the object which conforms to $J_i^T F_i$ in Eq. (24) is decreased. Consequently the ellipsoids in Fig. 14~15 are smaller than the ellipsoid in Fig. 11~12.

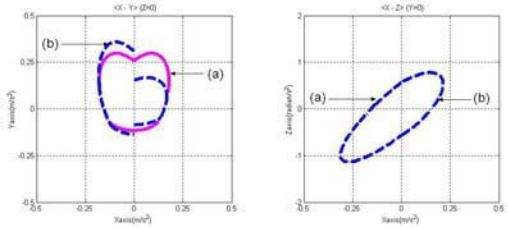

Fig. 14 Manipulability ellipsoid using class A and class B in Fig. 13
(a) Frictional contact with $\mu_1 = 0.5, \mu_2 = 0.5$
(b) Frictional contact with $\mu_1 = 0.3, \mu_2 = 0.7$

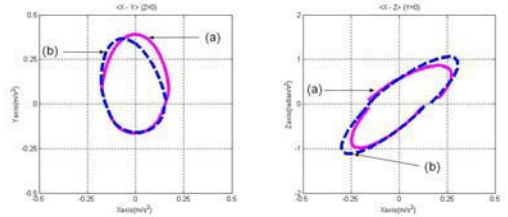

Fig. 15 Manipulability ellipsoid using class A and class C in Fig. 13
(a) Friction contact with $\mu_1 = 0.5, \mu_2 = 0.5$
(b) Friction contact with $\mu_1 = 0.1, \mu_2 = 0.9$

3. Case Study III

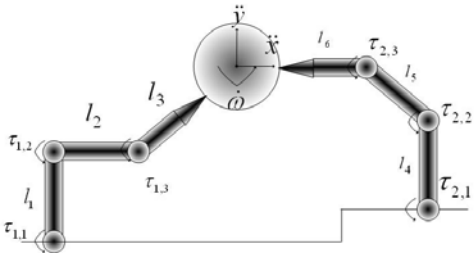

Fig. 16 Robot configuration of case III

The third application is the system consists of two three-link limbs grasping an object as Fig. 16. That is more general position than Fig. 13. When the robot configurations of $q_1 = 90^\circ, q_2 = -90^\circ, q_3 = 45^\circ, q_4 = 90^\circ, q_5 = 45^\circ, q_6 = 45^\circ$, $m_{1,2,3,4,5,6} = 1$, $l_{1,2,3,4,5,6} = 1$, $m_o = 1$, and $l_o = 1$ are given, this system is proper D.O.F. such that we use (26) and we get the result of Fig. 18.

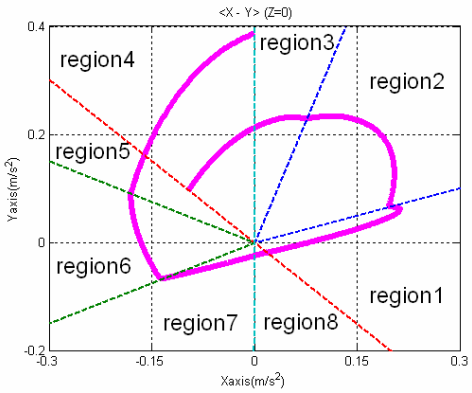

Fig. 17 Manipulability ellipsoid using class A and class B with $\mu_1 = 0.5, \mu_2 = 0.5$

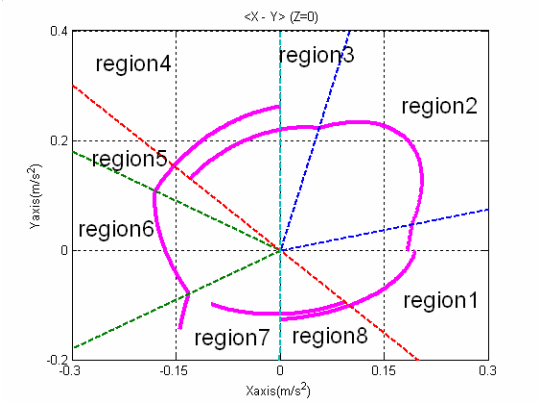

Fig. 18 Manipulability ellipsoid class A and class C with $\mu_1 = 0.5$, $\mu_2 = 0.5$

In region4 of Fig 17~18 which is equal to region4 of Fig. 3(c), both robot 1 and robot 2 can push the object (P_1P_2) alone and region3 exists outside of two friction cone ($\overline{C}_1\overline{C}_2$) such that whatever of robot 1 and robot 2 can carry the object.

Otherwise, in region8 of Fig 17~18 which is equal to region8 of Fig. 3(c), region8 is outside of two friction cone ($\overline{C}_1\overline{C}_2$) and neither robot 1 nor robot 2 can't carry the object ($\overline{P}_1\overline{P}_2$) alone such that no robot can push the object alone. Namely, two robots need to cooperate. When both robots push, force offset becomes internal force is and force which is not offset becomes external force. Acceleration of the object will be changed according as which robot makes external force. So region4 and region8 have two acceleration boundaries.

VI. Conclusion

In this paper, we analyze the effect of friction contact to robot manipulability ellipsoids. The system considered in the paper is comprised of multiple robots carrying a common object with frictional contacts. Internal forces play roles of generating friction force at each contact and the friction forces help each robot exert force to the object and carry the object without slip. Specifically, we introduced friction cone to the object acceleration workspace and apply the concept to the robot manipulability analysis. Based on the contact geometry and friction cones that determine slip-free region, we classify the workspace into three kinds of region. Different rules for determining specific relation between external forces and internal forces are developed for different class of region in workspace.

After connecting the object dynamics and robot dynamics, we derived the relation between robot joint torques and object acceleration for every class. After exerting constraint onto joint torques in 2-norm sense, we got a compounded elliptic geometry for object acceleration.

In distributing the forces to each robot, there are lots of ways to implement the required object motion. So, in future studies, we will try to answer the question: which distribution guarantees the maximum volume of acceleration.

Appendix

A. Dynamic Equation of Insufficient Degree of Freedom

A.1. Acceleration relationships between robots and object

We consider cases where the degrees of freedom of each robot are not sufficient to achieve arbitrary position/orientation in task space. To make the reduced Jacobian be invertible, we decompose Jacobian matrix into independent motion part and dependent motion part as $J = \begin{bmatrix} J^{ind} \\ J^{dep} \end{bmatrix}$ by exchanging the joint variables. With this decomposed Jacobian. That is

$$\dot{x}_i = \begin{bmatrix} J_i^{ind} \\ J_i^{dep} \end{bmatrix} \dot{q}_i \tag{29}$$

where J_i is constant matrix, so $\dot{J}_i$ is zero matrix, Therefore, differentiating (27) with respect to time yields.

$$\ddot{x}_i = J_i \ddot{q}_i = \begin{bmatrix} J_i^{ind} \\ J_i^{dep} \end{bmatrix} \ddot{q}_i, \quad \ddot{x}_i = \begin{bmatrix} \ddot{h}_i \\ \dot{\rho}_i \end{bmatrix} \tag{30}$$

where $\dot{\rho}_i$ is angular acceleration of end-effecter of robot i. From (16) and (29) we get transforming equation from $\ddot{q}_i$ to $\ddot{u}$.

$$\ddot{q}_i = \left[J_i^{ind}\right]^{-1} \ddot{h}_i = \left[J_i^{ind}\right]^{-1} B_i \ddot{u} \tag{31}$$

A.2. Connecting dynamic equation of object and robot

Putting (25), (27) and (31) into (26) and we get as:

$$\tau_i = \left[M_i \left[J_i^{ind}\right]^{-1} B_i + S_{i,1} K_i (HW)^{-1} HI_0\right] \ddot{u} \tag{32}$$

REFERENCES

[1] Yoshihiko Nakamura, "Advanced Robotics Redundancy and optimization", *Addison-Wesley Publishing Company*. 1991.

[2] T.Yoshikawa, "Analysis and Control of Robot Manipualtors with Redundancy", *Robotics Research, eds. M.Brady and R. Paul, MIT Press*, Cambridge, MA, pp. 734-745,1984.

[3] Jihong Lee, "Velocity Workspace Analysis for Multiple Arm Robot Systems. " *Robotica*, vol. 19, no. 5, vol. 5, pp. 581-591, Sep, 2001.

[4] Yoshikawa, T. Manipulability of robotic mechanisms. *Int. J. Robotics Res*. 4, 2 (1985), 3-9.

[5] J. K. Salisbury and B. Roth, "Kinematic and force analysis of articulated mechanical hands," *ASME J. Mech. Design,* vol. 82-DET-13, 1982.

[6] Antonio Bicchi, Claudio Melchiorri, and Daniele Balluchi, "On the Mobility and Manipulability of General Multiple Limb Robots," *IEEE Transactions on Robotics and Automation*, vol. 11, no. 2, pp. 215-227, 1995.

[7] Tsuneo Yoshikawa, "Dynamic manipulability of robot manipulators", *Journal of Robotic Systems*, vol. 2, no. 1, pp. 113-124, 1985.

[8] Oussama Khatib and Joel Burdick, "Optimization of dynamics in manipulator design: The operational space formulation," *The International Journal of Robotics and Automation*, vol. 2, no.2, pp. 90-98, 1987.

[9] Domenico Prattichizzo and Antonio Bicchi, "Dynamic Analysis of Mobility and Graspability of General Manipulation Systems," *IEEE Transactions on Robotics and Automation*, vol. 14, no. 2, April 1998.

[10] Tsuneo Yoshikawa, "Dynamic manipulabilitgy of robot manipualtors," *J. Robot. Syst.,* vol.2, no. 1, pp. 113-123, 1985.

[11] Jihong Lee and Hyungwon Shim, "Analysis of Acceleration Bounds of Cooperating Multiple Arm Robot Systems,", submitted to apear in *2004 IEEE/RSJ International Conference on Intelligent Robots and Systems.*